

# A stochastic model of discussion

S. Plaszczynski\*, B. Grammaticos, M. Badoual

Université Paris-Saclay, CNRS/IN2P3, IJCLab, 91405 Orsay, France

Université Paris-Cité, IJCLab, 91405 Orsay France

## Abstract

We consider the duration of discussions in face-to-face contacts and propose a stochastic model to describe it. It is based on the points of a Levy flight where the duration of each contact corresponds to the size of the clusters produced during the walk. When confronting it to the data measured from proximity sensors, we show that several datasets obtained in different environments, are precisely reproduced by the model fixing a single parameter, the Levy index, to 1.15. We analyze the dynamics of the cluster formation during the walk and compute analytically the cluster size distribution. We find that discussions are first driven by a maximum-entropy geometric distribution and then by a rich-get-richer mechanism reminiscent of preferential-attachment (the more a discussion lasts, the more it is likely to continue). In this model, conversations may be viewed as an aggregation process with a characteristic scale fixed by the mean interaction time between the two individuals.

**Keywords:** random walk, Levy flight, preferential attachment, face-to-face interactions

## 1. Introduction

Communication networks as face-to-face ones are described by time-varying graphs which are difficult to characterize because of the intertwining of the topological and temporal aspects [1, 2]. However, the sociological mechanisms that drive people encounters may actually be different from the ones that are involved when two individuals actually “interact”. Since in the following we only consider cases where people are face-to-face for at least 20 s, this means for humans that a *discussion* is engaged. It could follow some universal rules that lie out of the social context as stipulated in the field of Conversation Analysis [3]. This is suggested by a recent analysis [4] of the *sociopatterns* data (see *SM-SI* for their description). It was shown there that while the mean-time we spend together with a given person varies according to our preferences but also to the sociological context, the *deviations* from it seem to present a universal distribution. Most often we tend to allocate short times to our exchanges with a given individual (with respect to the usual mean-time) but very long discussions may emerge. What is remarkable is that the statistical distribution of this deviation, in particular for large values, looks the same in very different environments as between scientists at a conference or between farmers in a small Malawi village. This could point to some general properties of human face-to-face interactions, or more generally of primates since similar results were observed in a baboon population [4].

We try to model here the invariant distribution observed on what was called the “contact duration contrast” (or simply “con-

trast”) which is simply, for each relation (pair of individuals), the duration of contact divided by its mean-time. We have little indication on how to build such a model but we may rely on a very common mechanism that was dubbed “preferential attachment” in network science [5]. Introduced to explain the emergence of power-law degree distributions in real-life networks [6, 7, 8], it has in fact been studied by scientists under different forms since a century [9, 10, 11]. It is even known in common language, as “Matthew effect”<sup>1</sup>. It formalizes the idea of the “rich get richer” effect. For instance

- when a paper is abundantly cited, it is more likely to be known by others and thus cited even more [11, 5]. In the same vein, the more someone gets social rewards the more it is likely to be known by others and receive even more [12].
- in the so-called Yard-Sale model [13] a pair of agents bets a fraction of wealth of the poorest of the two with *equal probability to win*. Running such a system with several agents, the pairs being randomly selected, finally leads to “oligarchy”, i.e. a single agent concentrates all the wealth [14]. This is due to a rich-get-richer effect; when there is imbalance, it is less risky for the rich to bet some small amounts than for the poor, which further accentuates imbalance.
- in colloidal solutions, the more an aggregate grows, the more it is likely to be hit by particles and become even larger.

\*Corresponding author

Email address: stephane.plaszczynski@ijclab.in2p3.fr (S. Plaszczynski)

<sup>1</sup>Because of the sentence in the Bible “For unto every one that hath shall be given, and he shall have abundance [...]” (Matthew 25:29)

Discussions also hold a preferential-attachment mechanism. Everyone experienced that *when a conversation lasts for long, it is likely to last even more*. One can hardly escape it since there are more and more potential topics to come back to.

We propose a model to describe the dynamics of the discussion evolution, initially motivated by a coincidence on the shape between two distributions. It is based on geometric graphs build from the points of a Levy walk [15] that are first reviewed in sect. 2. Then we tune our empirical model to investigate at which level it can match the *sociopattern* data in sect. 3. This single-parameter model gives excellent results. Investigating the dynamics of clusters formation we show analytically why in sect. 4. Since the process we propose resemble that of a growing network [16], we compare them in more details in sect. 6. Finally in sect. 7, we comment on the geometric nature of the model and emphasize why, in the class of all random-walks, only Levy flights can be suitable candidates to model discussions through a geometric graph. Appendix A explains what the self-similarity of a Levy flight precisely means, and why it gives rise to several scaling relations in Levy graphs. Some auxiliary results are available in the Supplementary Material (SM).

## 2. Levy flights, graphs and clusters

A Levy flight, as introduced by B. Mandelbrot [17, 18] is a random-walk process but unlike the standard case where each step follows a Gaussian distribution (or converges to it due to the Central Limit Theorem, CLT), the length of the jumps follow a power-law distribution, namely a Pareto-Levy one [19]. The probability for a step length to exceed some value  $R$ , i.e. the complementary cumulative density function (CCDF) is

$$P(r > R) = \begin{cases} 1 & \text{if } r \leq r_0, \\ (r_0/R)^\alpha & \text{otherwise.} \end{cases} \quad (1)$$

$r_0$  is a cutoff that ensures the proper probability density function normalization, and  $0 \leq \alpha \leq 2$  is called the Levy index. In the following we will work in units of  $r_0$  so that, without loss of generality, we set  $r_0 = 1$ . We emphasize that the step length is always larger than  $r_0 = 1$  as is more apparent on the the probability density function

$$f(r) = \frac{\alpha}{r^{\alpha+1}} \Theta(r-1), \quad (2)$$

where  $\Theta$  is the Heaviside step function.

This power-law form implies infinite variance and also in some cases ( $\alpha \leq 1$ ) infinite expectation value. The random walk, i.e. the cumulative sum of independent steps distributed this way, fail the CLT and does *not* converge to a Gaussian distribution. Instead, following the work of P. Levy [20, 21], it was shown that it has a basin of attraction to what is known as  $\alpha$ -stable distributions (see e.g., [22]). This is called the Generalized Central Limit Theorem [23, 24] (the Gaussian case is recovered for  $\alpha = 2$ ).

A Levy flight can be simulated in a space of any dimension by drawing isotropically a direction, and a radial part following eq. (1). We will mostly focus our attention on dimension 2,

since it is the dimension for which the model best describes the data. In this case, the probability to return close to a previous point of the walk, which we loosely call the “return-probability” is most important.

The Levy flight trajectory has a fractal dimension  $\alpha$  [25]; the mean density of points within a sphere of radius  $R$  localized on one of the point of the flight, varies as  $1/R^{2-\alpha}$  [17, 15]. The process is statistically *self-similar*; loosely speaking the pattern of points “looks the same” at any scale. A more precise description is given in Appendix A. We will see that, due to this self-similarity, several power-law distributions (scaling relations) emerge. An introduction to the (rich) theory of Levy flights is given in [26].

A distinct feature of Levy flights is their clustering properties. Several points of the walk end nearby before a long jump triggers the construction of another cluster. Because of the absence of scale in eq. (1) a nested hierarchy of self-similar clusters is created [27]. To study quantitatively the clusters’ properties we need however to apply some scale. This can be performed by joining pairs of points which are below some distance  $s$  to form the edges of a geometric graph. The effect of applying explicitly a scale onto a scale-free process was studied in [15] and lead to a family of graphs  $\mathcal{L}_\alpha(s)$ , called “Levy Geometric Graphs”. They consist in a set of connected-components that we call (Levy) “clusters”. An example is show in Fig. 1. Although not (yet) justified, it was noticed that the mean number of clusters for a Levy graph of size  $N$  scales as

$$\langle N_c \rangle / N = A_c / s^{\alpha_c}, \quad (3)$$

where  $A_c \rightarrow 1$ ,  $\alpha_c \rightarrow \alpha$  in a large dimension space, and are obtained from numerical simulations otherwise (SM-S2).

## 3. An empirical model of discussion

An intriguing fact is that the cluster size contrast for Levy graphs (Fig.8 of [15]), i.e.  $n_i/\bar{n}$  where  $n_i$  denotes the size of the connected components, has a distribution that looks similar to what is observed for the duration of contacts in the *sociopatterns* data (Fig.4 of [4]). We thus try to match a model based on Levy graphs to the description of the observed duration contrast. To this purpose, on each *sociopatterns* dataset, we extract the set of all relations  $r$  and compute their total  $w(r)$  and mean  $\bar{t}(r)$  interaction time. Then, for each relation we generate a 2D Levy graph of size  $N = w(r)$ <sup>2</sup>. To match the observed mean-time to the mean cluster size we use eq. (3)

$$\langle N_c \rangle / N = 1/\bar{n} = A_c / s^{\alpha_c} = 1/\bar{t}, \quad (4)$$

which sets the scale to

$$s(r) = [A_c \bar{t}(r)]^{1/\alpha_c}, \quad (5)$$

where the  $A_c(\alpha)$  and  $\alpha_c(\alpha)$  values are taken from SM-S2. We then extract the connected-components of the graph and measure their size ( $n_i$ ) and compute the cluster size contrast  $\delta_i =$

<sup>2</sup>Since we use raw data,  $w(r)$  is expressed in units of the resolution step and has thus an integer value.

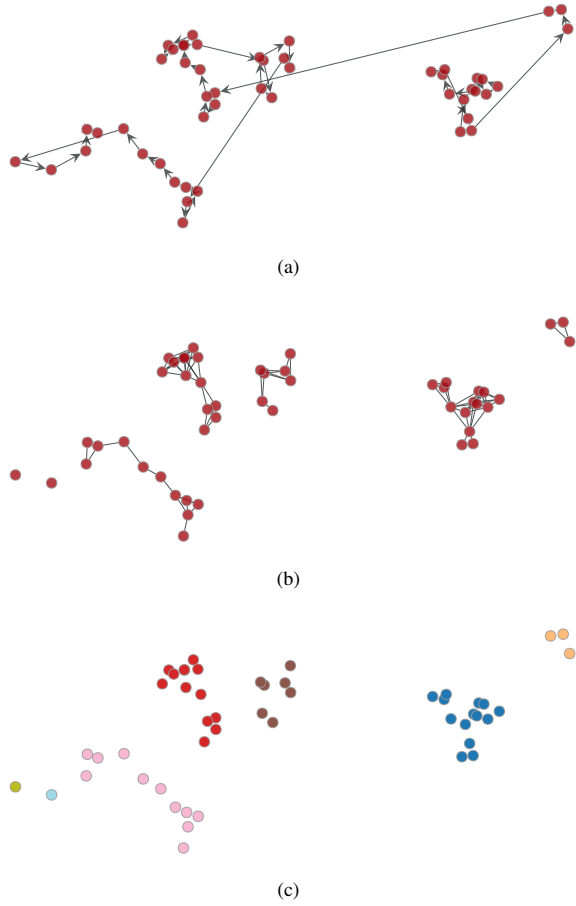


Figure 1: Example of construction of Levy clusters. (a) Levy flight. The points are obtained from a random Levy walk of index  $\alpha = 1.1$  and the line shows their creation path. (b) Levy graph. The points form the vertices of a graph with edges connecting pairs if their distance is inferior to the scale  $s$  (here  $s = 3$ ). (c) The connected components of the graph form Levy clusters which are colored the same. In our model, their size represent the duration of contact between two individuals and the scale is related to their interaction mean-time.

$n_i/\bar{n}$  distribution. Since the graph is random, we repeat the procedure 10 times and superimpose the results. The only free parameter in the model is the Levy index  $\alpha$ .

We show how the distributions vary for some  $\alpha$  values on the upper part of Fig. 2. There is little spread among the different realizations and, as shown in the bottom part of Fig. 2, a value around  $\alpha = 1.1$  reproduces well the data (a more precise determination will be given later).

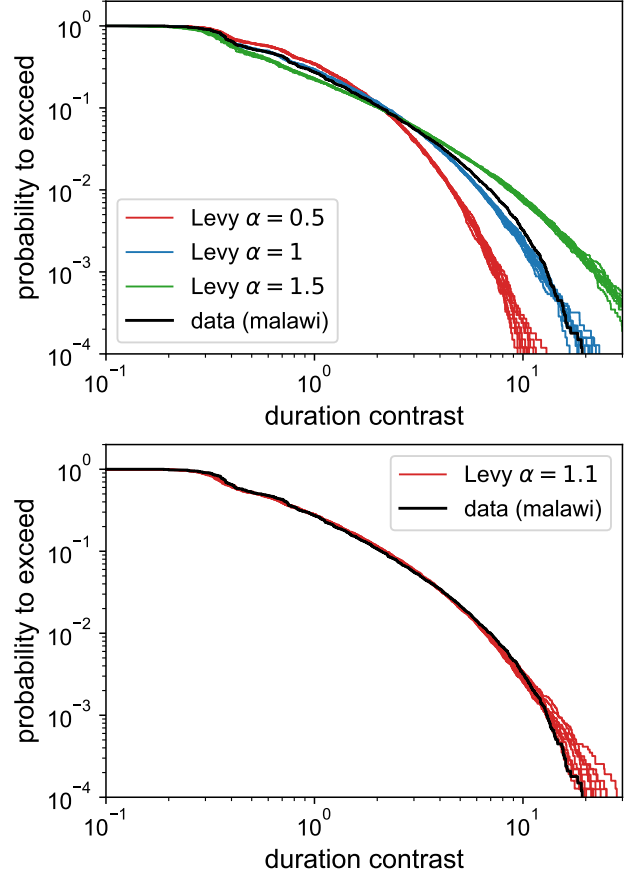


Figure 2: Upper: Comparison between the cluster size distribution contrast (CCDF) of the Levy model defined in the text for 3 indices ( $\alpha = 0.5, 1, 1.5$ ) and the contact duration contrast measured from the *sociopatterns* data recorded in a Malawi village [28]. Each line of the same color represents a different realization of the random graph. Lower: the best agreement is observed for  $\alpha = 1.1$ .

We then show in Fig. 3 that the same model accommodates also perfectly three other *sociopatterns* datasets while they were taken in some very different sociological environments (see *SM-SI* for details). It is remarkable that such a level of agreement is met on all the datasets *with the very same index* (which is the only parameter in the model). Even the tiny fluctuations at low contrast are well reproduced. While the fact that the data distributions are similar is already known (it is the main topic of [4]), the Levy graphs are built from very different set of relations and characteristics (interaction rates and mean-time). Thus the graphs' size and scale vary greatly between the datasets and it is not a trivial result that the same index can match the differ-

ent datasets nor that the low-contrast part can be reproduced so well.

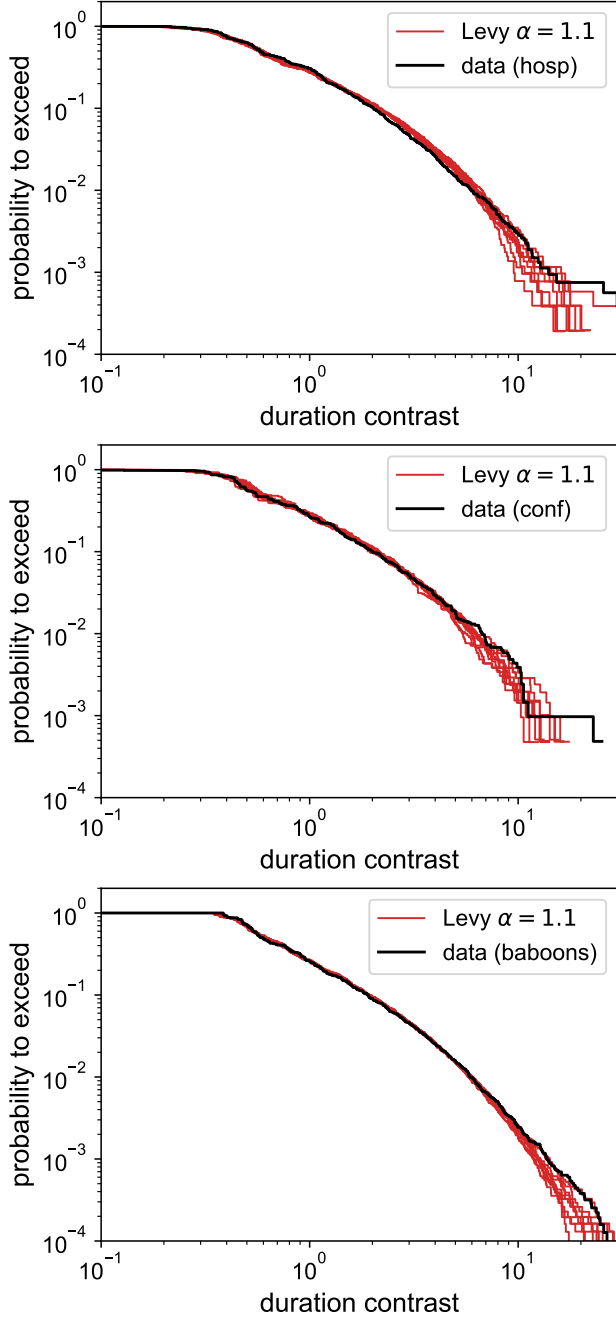


Figure 3: Comparison between the cluster size distribution contrast of the Levy model with a  $\alpha = 1.1$  index and the contact duration contrast measured on several very different *sociopatterns* datasets. Upper: in a french hospital, middle: at an international conference, lower: between baboons in an enclosure.

#### 4. Justification of the model

Although the agreement of the model with the data is impressive, it clearly lacks justification. To this purpose we need

to understand how clusters form during the evolution of the Levy flight, i.e. the dynamic of clusters formation in this peculiar form of random-walk. We proceed thus to computing analytically the distribution of the clusters size for any Levy geometric graph which will be shown to be of stretched exponential type.

##### 4.1. The dynamics of Levy clusters formation

We consider how clusters grow in a Levy graph when new points enter the flight. Fig. 4 shows some typical cases for the clusters growth.

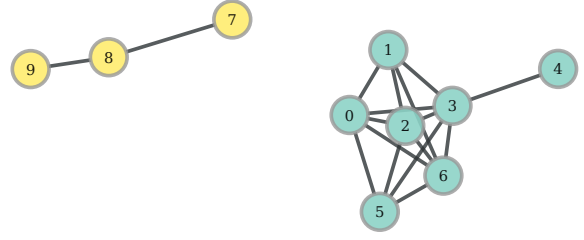


Figure 4: Example of two clusters obtained on a  $\mathcal{L}_1(3)$  graph. The numbers indicate the order of appearance of the points during the flight. Points are colored according to the cluster they belong to. The edges show pairs connected when their distance is below  $s = 3$ .

- The yellow cluster consists of three points (7,8,9), each being connected to the previous one. This is a case where the distances between the consecutive steps all fall below the chosen scale (here  $s = 3$ ). For reasons that will become clear later we call this the *geometric configuration*.
- The light-blue cluster (0,1,2,3,4,5,6) shows a more evolved configuration. Points are linked to their predecessors but for the (4-5) pair where the distance exceeds the scale. Point (5) is however close enough to (0), and later to (6), to be incorporated into the cluster. This effect is due to what we call the *return (or trapping) probability* which increases when there are more points. It is a “rich-get-richer” mechanism which will be investigated later.

Although both aspects are intimately related, we consider them first separately in order to understand their properties.

##### 4.1.1. The geometric case

Let us imagine that we can switch off the angular part in the jumps keeping only the radial distribution eq. (1). This is in fact possible, by performing a Levy flight on a 1D line but always in the same direction. One can approach also this regime by increasing the dimensionality of the space. Indeed in many dimensions it becomes very unlikely that a new jump connects to a previous point of the walk since it will most often go into other parts of the space. Let us call a “success” a jump that exceeds the distance  $s$ . Without a return probability, the only way to form a cluster is by linking the new point to the previous

one. To form a cluster of size  $n$ , one then needs  $n - 1$  consecutive “failures”. The corresponding probability is the geometric distribution

$$\mathcal{G}(n) = p_0(1 - p_0)^{n-1}, \quad (6)$$

where  $p_0$  is the probability to escape the cluster, which, according to eq. (1), is

$$p_0 = 1/s^\alpha, \quad (7)$$

and  $n$  starts at 1 (the minimal cluster size). The expectation value for the size of a cluster is

$$\mathbb{E}[n] = 1/p_0 = s^\alpha, \quad (8)$$

in agreement with eq. (3) for a large dimension space, since the mean number of clusters in a graph of size  $N$  is  $\langle N_c \rangle = N/\langle n \rangle$ . We show in Fig. 5, using simulations, that when increasing the dimension of the space for the Levy flight, the cluster size distribution converges indeed to the geometric one.

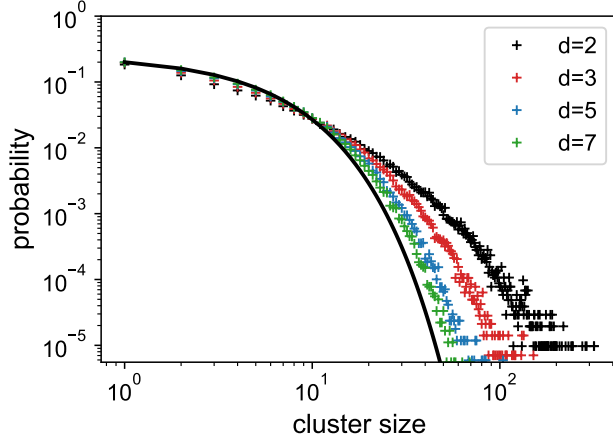


Figure 5: Distribution of the clusters size for a  $\mathcal{L}_1(5)$  graph obtained by simulation ( $N = 10^6$  steps) increasing the space dimensionality  $d$  (points). The distributions converge to the geometric form (black line).

We now consider the walk in dimension 2 where the effect of the return-probability cannot be neglected especially for large clusters (Fig. 5). To gain intuition on its effect on cluster formation we would like to cancel the geometric configuration. This may be performed in the following way. Remembering that a single Pareto-Levy step always produces a point at a distance beyond  $r_0 = 1$  (eq. (2)), if we construct a Levy graph at a scale  $s = 1$  or below, two consecutive points can never get connected. Without a return probability, this would lead only to a set of singlet clusters. However the return-probability brings back some points from the walk close to previous ones opening the possibility to create Levy clusters with more than a single vertex. Fig. 6 shows the resulting distributions obtained in simulations with a scale  $s = 1$  and varying the Levy index. They fall steeply and converge to a power-law as  $\alpha$  reaches 2, which will be confirmed analytically later. The emergence of heavy tails that are close to power-law ones is typical of a preferential-attachment mechanism that we shall now investigate.

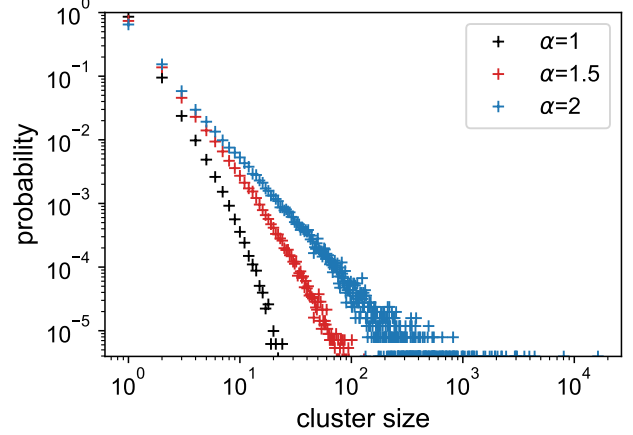


Figure 6: Distribution of 2D Levy clusters size with a scale  $s = 1$  for  $\alpha = 1, 1.5$  and 2.

#### 4.1.2. Preferential attachment

As presented in the introduction, discussions benefit from a preferential attachment effect: when they last for long it is likely they will extend even more. It becomes more and more difficult to escape a conversation while it lasts. This feature is captured in our model by the Levy clusters. When the size of a cluster increases, its trapping probability increases too; it gets more and more difficult to *escape the cluster*, i.e. fall in a region of the space far from the cluster points. We may get an order of magnitude of this effect with the following argument. In 2D in average,  $k$  points in a cluster occupy an area  $\pi R_c^2$ , so that the mean cluster radius varies as  $R_c \propto \sqrt{k}$ . The probability to escape the cluster with a single step, i.e. perform a step beyond  $R_c$  is then of the order of (see eq. (1))

$$p(r > R_c) \propto \frac{1}{k^{\alpha/2}}. \quad (9)$$

While  $k$  increases the success probability (to escape the cluster) decreases. A cluster of size  $n$  occurs when there are  $n$  consecutive failures. We thus generalize the geometric form eq. (6) to

$$p(n) \propto \prod_{k=1}^n (1 - p_0(k)), \quad (10)$$

where

$$p_0(k) = \frac{A}{k^\gamma}, \quad (11)$$

and  $\gamma$  should be close  $\alpha/2$ . The normalization is given by  $\sum_n p(n) = 1$  and the geometric configuration is recovered by canceling the preferential attachment term with  $\gamma \rightarrow 0$  and  $A \rightarrow p_0 = 1/s^\alpha$ .

We confront this formula to the measured cluster sizes obtained in simulations, performing a least-squares minimization on  $A$  and  $\gamma$ , for several values of  $\alpha$  and  $s$  varied in the range  $0.8 \leq \alpha \leq 1.4$  and  $3 \leq s \leq 10$ . We obtain an excellent agreement in each case as shown on some examples in Fig. 7.

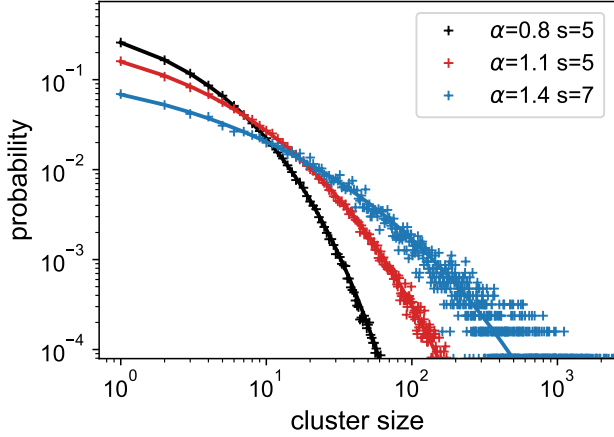


Figure 7: Clusters size distribution obtained from Levy graphs simulations for some  $\alpha$  and  $s$  values (points). The curves show the corresponding eq. (10) model, adjusting the  $A$  and  $\gamma$  parameters with least-squares minimization.

We now consider the values of  $\gamma$  and  $A$  extracted from the fits. As shown in Fig. 8 the exponent  $\gamma$  depends essentially on  $\alpha$  and at large scales (corresponding to large  $R_c$  in eq. (9)) converges indeed to  $\alpha/2$ .

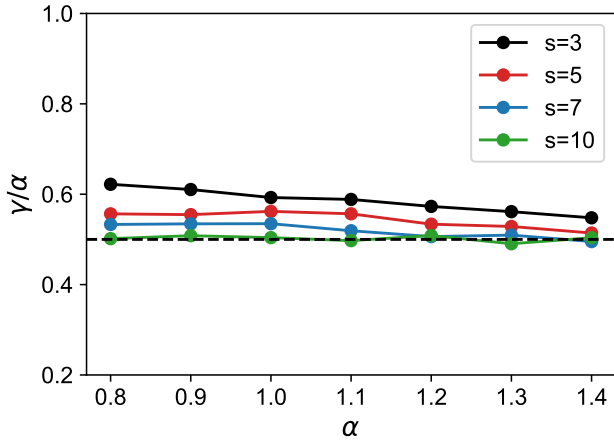


Figure 8: Ratio between the  $\gamma$  parameter of eq. (10) and  $\alpha$  determined from  $\mathcal{L}_\alpha(s)$  simulations varying  $\alpha$  for several scales  $s$ . The dashed line at 0.5 represents the eq. (9) expectation.

On the contrary, the amplitude term  $A$  mostly depends on the scale as shown in Fig. 9 with a power-law dependency of the form

$$A(s) = c/s^\beta. \quad (12)$$

The  $c$  and  $\beta$  coefficients are obtained from simulations (SM-3) and for  $\alpha$  around 1 are described by

$$c = 1.19 + 0.31\alpha \quad (13)$$

$$\beta = 0.57 + 0.14\alpha, \quad (14)$$

with a  $\pm 0.02$  precision on each parameter. For the discussion model  $c = 1.5, \beta = 0.7$ .

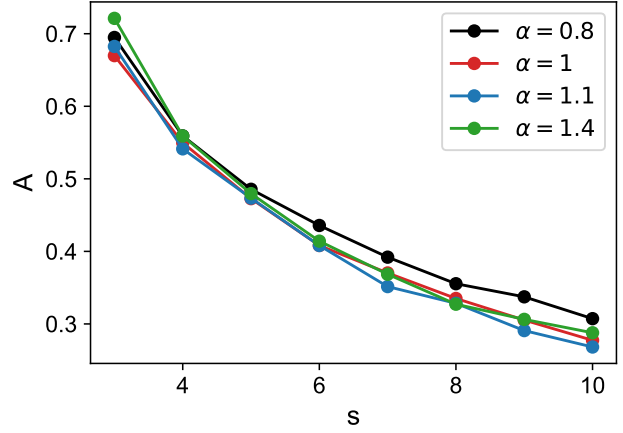


Figure 9: Value of the amplitude term  $A$  in eq. (10) determined from simulations as a function of the scale  $s$  for several  $\alpha$  values.

We thus have the whole description of the clusters size probability function

$$p(n; \alpha, s) \propto \prod_{k=1}^n \left(1 - \frac{c}{s^\beta k^\gamma}\right), \quad (15)$$

which may be further simplified. Since

$$p(n)/p(n-1) = 1 - A/n^\gamma, \quad (16)$$

the logarithmic slope goes asymptotically as

$$D = \frac{\ln p(n) - \ln p(n-1)}{\ln n - \ln(n-1)} \sim -An^{1-\gamma}, \quad (17)$$

with  $\gamma \simeq \alpha/2$ . For  $\alpha = 2$  we obtain a pure power-law form as was observed in Fig. 6. Considering the continuum case,  $D = \frac{n}{p} \frac{dp}{dn}$ , we find that, for  $\alpha < 2$ , the distributions follows asymptotically that of a stretched exponential

$$p(n) \propto \exp\left(-\frac{A}{1-\gamma} n^{1-\gamma}\right). \quad (18)$$

Numerically it appears that this approximation is in fact good on the whole range of cluster sizes as shown in Fig. 10.

The distribution for the discussion model is

$$p(n; \alpha = 1.1, s \gg 1) \propto \exp\left(-\frac{3.3}{s^{0.7}} n^{0.45}\right). \quad (19)$$

The generalization to a space of any dimension can be easily performed. Adapting the argument leading to eq. (9) to a ball in a  $d$  dimensional space

$$\gamma = \alpha/d. \quad (20)$$

When changing the dimension, the parameters  $c$  and  $\beta$  of the amplitude term  $A = c/s^\beta$  evolve but the asymptotic expression eq. (18) still holds as shown in the SM-S4. When  $d$  increases  $\gamma \rightarrow 0$  and  $c \rightarrow 1, \beta \rightarrow \alpha$  and the cluster size distribution converges to  $\exp(-n/s^\alpha)$  which is the continuous extension of the geometric function as was observed in Fig. 5.



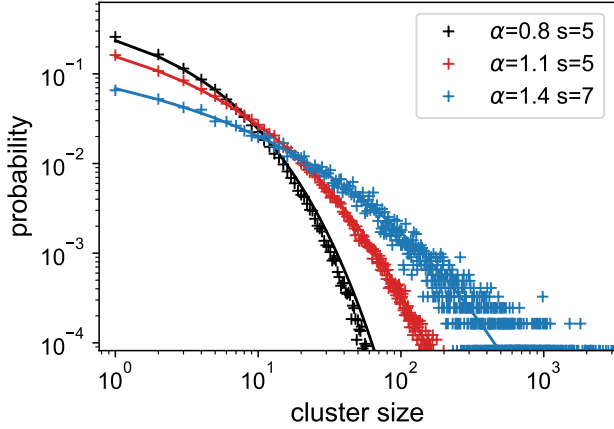


Figure 10: Distribution of the clusters size (points) compared to the stretched exponential model eq. (18) derived in the text (lines).

#### 4.2. Scaling relations

We may now compute the mean cluster size using the asymptotic expression. With the shorthand notations  $\mu = 1 - \gamma$ ,  $\lambda = A/\mu = c/(\mu s^\beta)$

$$\bar{n} = \frac{u}{v} = \frac{\int_1^\infty n e^{-\lambda n^\mu} dn}{\int_1^\infty e^{-\lambda n^\mu} dn}. \quad (21)$$

With the change of variable  $t = \lambda n^\mu$  the denominator becomes

$$v = \frac{\lambda^{-1/\mu}}{\mu} \Gamma(1/\mu, \lambda), \quad (22)$$

where the incomplete  $\Gamma$  function is defined by

$$\Gamma(a, z) = \int_z^\infty t^{a-1} e^{-t} dt. \quad (23)$$

Integrating by parts and performing a similar computation on the numerator yields

$$u = \frac{\lambda^{-2/\mu}}{\mu} \Gamma(2/\mu, \lambda^2), \quad (24)$$

and the mean number of clusters finally reads

$$\bar{n} = \frac{\lambda^{-1/\mu} \Gamma(2/\mu, \lambda^2)}{\Gamma(1/\mu, \lambda)}. \quad (25)$$

When the scale increases  $\lambda = c/(\mu s^\beta) \rightarrow 0$  and asymptotically the mean cluster size scales with  $s$  as

$$\bar{n} = \frac{\Gamma(2/\mu)}{\Gamma(1/\mu)} \left(\frac{\mu}{c}\right)^{1/\mu} s^{\beta/\mu}, \quad (26)$$

This regime is however only reached for very large scales ( $s \gtrsim 10$ ). Although the  $\Gamma(2/\mu, \lambda^2)$  function in the numerator of eq. (25) converges rapidly to  $\Gamma(2/\mu)$ , this is not the case for  $\Gamma(1/\mu, \lambda)$  in the denominator with  $\beta \simeq 0.7$ . Numerically the

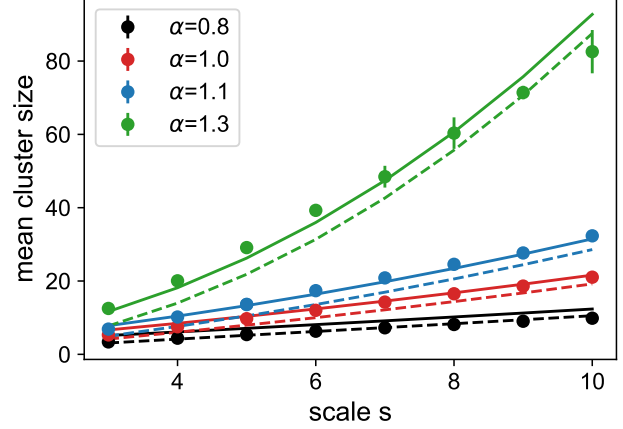


Figure 11: Mean clusters size of  $\mathcal{L}_\alpha(s)$  graph's measured on the simulation (points) varying the scale for a few  $\alpha$  values, compared to the exact analytical model eq. (25) (full lines) and its approximation eq. (26) (dashed lines).

variation of this term with  $s$  in a limited scale range is smooth and leads essentially to a constant correction term in eq. (26). This is shown in Fig. 11 where we compare the results from simulations to eqs. (25) and (26). The agreement is good given the uncertainties on the fitted  $\gamma$ ,  $c$  and  $\beta$  parameters.

Because of the long jumps in the Levy walk, the formation of a cluster at a given scale is essentially a *local* process. The walker almost never “comes back” to a previous cluster after a long jump. Clusters are thus mostly *uncorrelated* and Levy graph's may be viewed as a “factory” of clusters. The sum of sizes of the  $N_c$  clusters equals the graph's size

$$\sum_{i=1}^{N_c} n_i = N. \quad (27)$$

In the mean, each (independent) cluster contributes to  $\bar{n}$  so that  $\langle N_c \rangle \bar{n} \simeq N$ . This explains the origin of the second scaling law on the fractional number of clusters (eq. (3))

$$\langle N_c \rangle / N \simeq 1/\bar{n} \propto 1/s^{\beta/\mu}. \quad (28)$$

#### 4.3. The cluster size contrast distribution

We now have all that is needed to compute analytically the distribution of the cluster size contrast variable  $\delta = n/\bar{n}$ , as observed in Figs. 2 and 3. Performing the change of variable  $n \rightarrow n/\bar{n}$  using eqs. (18) and (26) and normalizing the result, we obtain

$$p(\delta) = \frac{\mu \Gamma(2/\mu)}{\Gamma^2(1/\mu)} e^{-\left[\frac{\Gamma(2/\mu)}{\Gamma(1/\mu)} \delta\right]^\mu} \quad \text{with } \mu = 1 - \frac{\alpha}{2}. \quad (29)$$

Integrating the formula, we obtain the CCDF

$$\begin{aligned} p(\delta > x) &= \int_x^\infty p(\delta) d\delta \\ &= \frac{\Gamma[1/\mu, (x \Gamma(2/\mu)/\Gamma(1/\mu))^\mu]}{\Gamma(1/\mu)} \end{aligned} \quad (30)$$

where the incomplete  $\Gamma$  function is given by eq. (23).

For the discussion model we have

$$p(\delta) = 3.9 e^{-2.8\delta^{0.45}}, \quad (31)$$

$$p(\delta > x) = 0.9 \Gamma(2.2, 2.8x^{0.45}). \quad (32)$$

We show in Fig. 12 the agreement of this formula with simulations. We also added the contrast distribution of the Geometric contribution which is [15]

$$p(\delta > x) = (1 - p_0)^{x/p_0}. \quad (33)$$

It shows that short discussions are rather driven by the geometric term while the tail arises from the preferential-attachment mechanism.

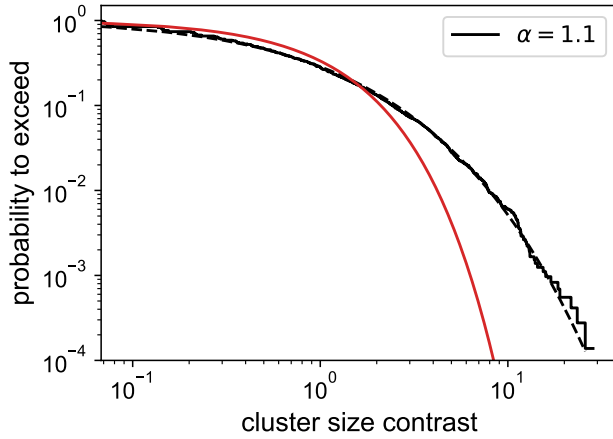


Figure 12: Distribution of the cluster size contrast for the discussion model based on a Levy graph of index 1.1. The full black line represent the CCDF measured from simulations and the dashed one the analytical formula derived in the text (eq. (31)). The red curve corresponds to the geometric contribution.

## 5. The Levy index

We can now determine the value of the Levy index on the *sociopattern* datasets. The analytical expression for the contrast distribution, eq. (29), must however be refined in order to build a precise likelihood function by taking into account two effects.

- First, eq. (29) was derived for large scale values. Because of the low resolution of the *sociopattern* data ( $T=20$  s), the scales of the Levy graphs cover a rather low range ( $1 \lesssim s \lesssim 2$ ). Furthermore it was shown that the mean cluster size that is used in the computation (eq. (26)) is slightly underestimated. To account for both effects we add a normalizing factor  $f$  that we compute from simulations so as to reproduce precisely the contrast distribution measured on Levy graphs. It is of the order of 1.3 depending on the dataset (details in SM-S5).
- Second, eq. (29) was derived asymptotically and since we are mostly interested in the tail of the distribution we consider samples above  $\delta_{min} = 2$  (similar results are obtained

with  $\delta_{min} = 3$ ). Care must then be taken on normalizing the likelihood accordingly (as in [29]).

The improved contrast distribution reads

$$p(\delta; \alpha) = \frac{g\mu}{\Gamma(1/\mu, (g\delta_{min})^{1/\mu})} e^{(-g\delta)^\mu} \quad (34)$$

$$\text{with } \mu = 1 - \alpha/2, \quad g = f \frac{\Gamma(2/\mu)}{\Gamma(1/\mu)}. \quad (35)$$

The likelihood function for the set of measured values  $\delta_i > \delta_{min}$  is

$$\mathcal{L}(\alpha) = \prod_i p(\delta_i, \alpha). \quad (36)$$

Fig. 13 shows the normalized likelihood functions on the four datasets.

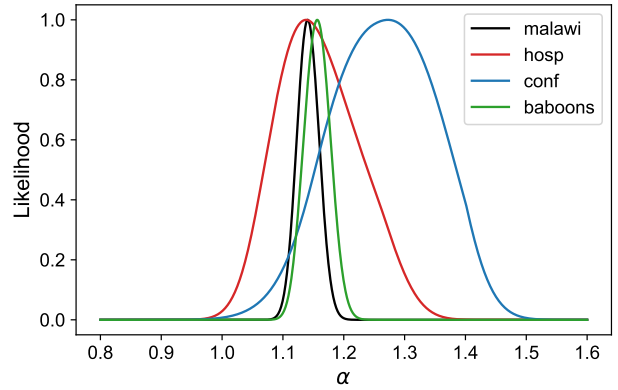


Figure 13: Likelihood functions eq. (36) measured on the *sociopattern* datasets.

The maxima of these functions gives the maximum likelihood estimate of the Levy index  $\hat{\alpha}$  and the width of the support indicates the statistical precision of the estimator. To take also into account the stochastic nature of the model (based on random graphs) we use simulations. For each dataset, we generate 100 realizations of the corresponding Levy graphs, compute each time the maximum likelihood estimate and consider the spread of the resulting distribution (see SM-S5). This allows to obtain the standard deviation of the estimator and its 95% confidence level intervals. Results are given in Table 1. The Levy indices determined on each dataset are compatible and their combined value is  $\hat{\alpha} = 1.15 \pm 0.02$ .

## 6. Discussions as an aggregation process

Our model somewhat resembles that of a growing network with a sub-linear (power-law) kernel [16] In this model, nodes are added sequentially and attached to previous ones with a probability related to their connectivity  $p(k) \propto k^\gamma$ . Asymptotically, the average number of sites with  $k$  links grows up linearly  $N_k(t) = tn_k$  and [16]

$$n_k = \frac{\mu}{k^\gamma} \prod_{j=1}^k \left(1 + \frac{\mu}{j^\gamma}\right)^{-1}. \quad (37)$$



dataset	$\hat{\alpha}$	$\sigma$	95% CL
<i>malawi</i>	1.14	0.02	[1.11,1.18]
<i>hosp</i>	1.14	0.06	[1.07,1.26]
<i>conf</i>	1.27	0.09	[1.12,1.39]
<i>baboons</i>	1.16	0.03	[1.10,1.20]

Table 1: Estimate of the Levy index for the different datasets.  $\alpha$  is the Maximum Likelihood Estimate,  $\sigma$  its standard deviation and the last column indicates the 95% confidence level interval.

There are some similarities with our model (eq. (10)) since for large  $j$  values  $(1 + \mu/j^\gamma)^{-1} \simeq 1 - \mu/j^\gamma$ . There are however also a number of important differences.

- By construction, the network has a single connected-component and  $k$  denotes the vertices degree.
- In growing networks, there is a single degree of freedom, the amplitude term  $\mu$  being related to  $\gamma$  and  $1 < \mu(\gamma) < 2$  which is not what we measure for our amplitude term (Fig. 9).
- The fact that there is a single cluster gives rise to the  $\mu/k^\gamma$  pre-factor which does not appear in eq. (10).

The analogy with a growing network is thus limited although both approaches lead to stretched exponential distributions. The discussion model should be rather considered as an aggregation process<sup>3</sup>. Two points get connected if their relative distance is below the scale  $s$ . This is equivalent to considering some disks of diameter  $s$  centered on each point that get connected if they overlap (see Fig. 14). Clusters/discussions between two individuals thus appear as aggregates of such disks with a natural radius determined by those persons mean-interaction time (eq. (5)). As the aggregate (discussion) grows, it gets more likely for the next jumps of the disk to “stick” to it (conversation continues) which illustrates again the preferential attachment mechanism.

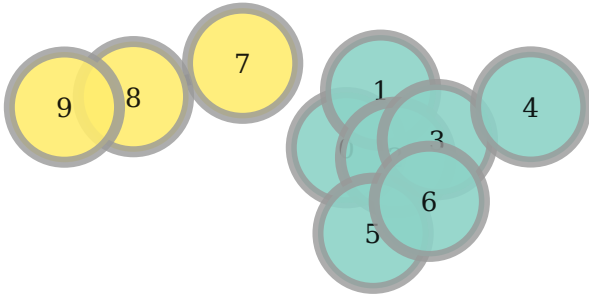


Figure 14: The formation of Levy clusters seen as an aggregation process. The Figure is the same as Fig. 4 when drawing disks of diameter  $s$  around each vertex. Each discussion corresponds to a colored aggregate.

<sup>3</sup>The difference between both processes was already outlined in [16].

## 7. Discussion(s)

We have computed analytically the cluster size distribution for any Levy geometric graph and found it to be of stretched-exponential type. But more importantly, we unraveled the mechanism by which clusters form and its analogy with the way discussions develop.

The initial phase is described by a geometric distribution, which for a large scale is the exponential one. For a fixed mean-value, it is the *maximum entropy* distribution [30, 31]. It means that, beside its mean-time, there is no *prior* information on the duration the conversation will take.

While more points are added to the cluster (discussion) it is more likely that the next ones will be linked (related) since geometrically the trapping probability increases. This is a preferential-attachment mechanism and reproduces the idea that as a discussion lasts it is more likely to last even more.

In this model, discussions appears as an aggregation process between “disks” with a natural size fixed by the (usual) mean-time of the relation. Considering a discussion as a form of aggregation sounds reasonable. Our main finding is that experimental data are very well reproduced when the disks follow a 2D Levy-flight of index  $\alpha = 1.15$ .

The duration of each discussion, characterized in the model by a number of points, is a *discrete* quantity expressed in units of the resolution step ( $T = 20s$  for the *sociopatterns* data). Obviously we want a model that is independent from that resolution. With a better instrument (lower  $T$ ) the duration and mean-time values would increase. In the Levy model this means changing the scale of the Levy graph (see eq. (5)) along with its number of points (size). Among the class of random-walks only a Levy flight is resolution-independent. Indeed, when increasing the scale of any geometric graph based on a standard (finite-variance) random-walk, we end-up with a single cluster, the giant component. When increasing the resolution, such a model would lead to a single conversation between the two individuals. On the contrary, Levy-walk based graphs escape percolation [15]. Increasing the scale, the size of the graph changes and there are still clusters. The important point is that the cluster size/duration contrast  $\delta = n/\bar{n} = t/\bar{t}$  is independent from the scale as was derived in eq. (29).

A (measured) value of  $\alpha = 1.15$  is nothing special in the class of Levy processes. Although there are some mathematical differences when crossing the value  $\alpha = 1$  [32] this value looks excluded. We note that several human activities exhibit a power-law dependency with an exponent around 1 (see e.g., [33, 34]) but keep in mind that our process is more elaborate than a mere power-law distribution. This could be a consequence of the “least effort principle”, as proposed by G. Zipf [35] to explain several scaling exponents around 1 related to human behavior (such as the word frequency), but a convincing explanation remains to be found.

The fact that the random walk is performed in a space of dimension 2 is only dictated by the data. A walk in a higher dimensional space fits the data less well (SM-S6).

A “point” in our model denotes a time-unit. It could be related to a notion of information or more generally to a “topic”

(or concept). In the geometric phase, which starts the discussion, each individual would discuss the initial topic, each one answering to the previous “point”. The return-probability would mean a break in this flow to a “point” previously raised. The preferential-attachment mechanism would mean that while more topics have been addressed it is more likely to get back to one of them. This is what is observed on internet discussion feeds [36]. A person (“A”) posts some question and gets an answer from “B”, and there might be an exchange between the two leading to a “A-B-A...” sequence. This is what we identify as the geometric phase. While the discussion goes on, third party users (“C”, then “D” etc.) may enter the game, by commenting some part of the discussion which leads to branches in the feed. The complexity of the discussion increases, sometimes to a point where the whole exchange gets out of control in solving the initial question. This evolution looks somewhat similar to what we observe in face-to-face discussions but there are some important differences too (there are for instance several participants in the feed). Testing whether such a hypothesis for the meaning of the word “point” makes sense requires the tools of Conversation Analysis [3].

## Conclusion

We have proposed a stochastic model to describe the duration of discussions between two individuals. It reproduces precisely the distributions of the contrast duration of contacts (i.e. the dimensionless deviation from the mean-value) on several datasets of face-to-face interaction recordings, with a single parameter, the Levy index, that was found to be  $\alpha = 1.15 \pm 0.02$ .

The model is based on some simple considerations about conversations. A discussion always starts about a topic that is first explored. While it lasts, it becomes more likely to last even more since there are more points to come back to. Such a behavior can be reproduced by considering the size of the clusters (connected components) in geometric graphs built from the points of a Levy flight, named Levy Geometric Graphs [15]. We derive analytically the cluster size distribution which is of stretched-exponential type. By dividing it by the mean-value to obtain the dimensionless “duration contrast” variable, we show that it becomes independent of the resolution. This is a necessary requirement for the model which cannot be met by any other type of random-walk. The analysis of the clusters dynamics reveals that they initially form by linking each point to the previous one (geometric phase). Then as more points are added more complex structure emerge due to the increasing return-probability to some previous points (preferential attachment).

We also show that while the model shares some similarities with the case of a growing network with a sub-linear kernel, it actually belongs to the class of aggregation processes. The model may be viewed as a “disk” with a diameter related to the mean-interaction time, that makes jumps following a Levy flight of index 1.15 (see Fig. 14). The size of each set of overlapping disks represents the duration of a discussion.

Finally we may question the very notion of discussion and language. We have disregarded the fact that baboon’s interaction shows dynamics similar to human one [4] and are thus also

characterized in our model by a Levy index of  $\alpha = 1.1$  (Fig. 3). Although our communication through an evolved verbal language is (probably) more complex than the baboons’ one, this calls into question the very notion of “discussion” and the role of language on the development of the human species [37].

## Appendix A. Levy flights self-similarity

To understand the origin of the scaling relations, we come back to the individual points of the Levy walk, that we label with time and consider as complex-valued,  $X(t)$ . Although the variance is formally diverging, one may get a similar quantity by rescaling the lower-order fractional moments [32]

$$\begin{aligned} \langle \|X(t)\|^q \rangle &\propto t^{q/\alpha}, \\ \langle \|X(t)\|^q \rangle^{2/q} &\propto t^{2/\alpha}, \end{aligned} \quad (\text{A.1})$$

where  $0 < q < 2$  for convergence. This pseudo-mean squared displacement reveals the super-diffusive nature of the walk, with a Hurst exponent (see e.g., [38])

$$H = 1/\alpha. \quad (\text{A.2})$$

This result may also be obtained on finite size samples [39] or using a sliding window during the walk [40] or more rigorously with a Renormalization Group approach [41]. Self-similarity corresponds to the fact that  $X(t)$  and  $X(rt)/r^H$  are statistically indistinguishable for any  $r$  value, i.e. that the samples follow exactly the same underlying distribution (we illustrate it with simulations in SM-S7). We note that  $X(t) \equiv X(rt)/r^H$ . Taking  $r = 1/s^\alpha$  and using eq. (A.2), we find that

$$X(t)/s \equiv X(t/s^\alpha), \quad (\text{A.3})$$

This relation shows that *rescaling* the random function random  $Y(t) = X(t)/s$  is equivalent to *sub-sampling* the original process by a factor  $1/s^\alpha$ . This is in line with the definition of the effective diffusion coefficient for a Weierstrass random walk [27], the analog of a Levy flight but on a square lattice of mesh size  $a$ , given by (see e.g., [22])  $D_{eff} = \lim_{a, \Delta t \rightarrow 0} a^\alpha / \Delta t$ .

A Levy graph of scale  $s$  is constructed by linking points satisfying  $\|X(t_i) - X(t_j)\| < s$  or using the rescaled variable  $\|Y(t_i) - Y(t_j)\| < 1$ . Changing the scale is equivalent to varying the graph’s size by  $N/s^\alpha$  but otherwise keeping topologically equivalent configurations. Then all statistics related to the graph’s size, vary with  $s^\alpha$ . For instance, the fraction of edges, average degree or mean cluster size all scale with  $s^\alpha$ . The number of clusters, being the inverse of the mean cluster size, eq. (28), scales inversely.

So why is the exponent we computed for the mean cluster size (eq. (26)) not exactly  $\alpha$  but a more complicated function of it? The reason lies in what we call the “Levy flight”. We have focused on the original definition given by Mandelbrot [17], not on the one used to derive eq. (A.1) which is based on steps following *exactly* a  $\alpha$ -stable distributions (as a Cauchy one for  $\alpha = 1$ ). The Pareto-Levy distribution used throughout the text (eq. (2)) is not exactly a stable one, because of the gap below

$r_0 = 1$ . However, because of the Generalized CLT [24], its cumulative sum (i.e. the random-walk) converges rapidly to it. While for most observables it has very little impact, it slightly affects the clusters size (which are often made up from the very first points of the walk) which makes the calculation of their distribution more elaborate.

## Acknowledgments

We thank Alexandre Delanoë for enlightening discussions on conversation analysis and the analogy with internet discussion feeds.

## Competing interests

The author declare no competing interests.

## Funding

Public research.

## Availability of data and material

- The datasets analyzed in this study are available from the *sociopatterns* repository, [www.sociopatterns.org](http://www.sociopatterns.org)
- The python3 software used to produce the results is available from <https://gitlab.in2p3.fr/plaszczynski/coll>
- All graph-related computations and figures were obtained with the graph-tool (v 2.43) software [42].

## References

- [1] P. Holme, J. Saramäki, *Temporal Networks*, Physics Reports 519 (3) (2012) 97–125, arXiv: 1108.1780. doi:10.1016/j.physrep.2012.03.001. URL <http://arxiv.org/abs/1108.1780>
- [2] P. Holme, *Modern temporal network theory: a colloquium*, Eur. Phys. J. B 88 (9) (2015) 234. doi:10.1140/epjb/e2015-60657-4. URL <http://link.springer.com/10.1140/epjb/e2015-60657-4>
- [3] G. Button, M. Lynch, W. Sharrock, *Ethnomethodology, Conversation Analysis and Constructive Analysis: On Formal Structures of Practical Action*, 1st Edition, Routledge, London, 2022. doi:10.4324/9781003220794.
- [4] S. Plaszczynski, G. Nakamura, B. Grammaticos, M. Badoual, *On the duration of face-to-face contacts*, EPJ Data Science 13 (1) (Jan. 2024). doi:10.1140/epjds/s13688-023-00444-z. URL <http://dx.doi.org/10.1140/epjds/s13688-023-00444-z>
- [5] R. Albert, A.-L. Barabási, *Emergence of Scaling in Random Networks*, Science 286 (5439) (1999) 509–512. doi:10.1126/science.286.5439.509. URL <http://dx.doi.org/10.1126/science.286.5439.509>
- [6] R. Albert, A.-L. Barabási, H. Jeong, *Mean-field theory for scale-free random networks*, Physica A: Statistical Mechanics and its Applications 272 (1–2) (1999) 173–187. doi:10.1016/S0378-4371(99)00291-5. URL [http://dx.doi.org/10.1016/S0378-4371\(99\)00291-5](http://dx.doi.org/10.1016/S0378-4371(99)00291-5)
- [7] P. L. Krapivsky, S. Redner, F. Leyvraz, *Connectivity of Growing Random Networks*, Physical Review Letters 85 (21) (2000).
- [8] S. N. Dorogovtsev, J. F. F. Mendes, A. N. Samukhin, *Structure of Growing Networks with Preferential Linking*, Physical Review Letters 85 (21) (2000).
- [9] F. Y. E., G. U. Yule, *A Mathematical Theory of Evolution Based on the Conclusions of Dr. J. C. Willis, F.R.S.*, Journal of the Royal Statistical Society 88 (3) (1925) 433. arXiv:10.2307/2341419, doi:10.2307/2341419.
- [10] H. A. Simon, *On a class of skew distribution functions*, Biometrika 42 (3–4) (1955) 425–440. doi:10.1093/biomet/42.3-4.425.
- [11] D. D. S. Price, *A general theory of bibliometric and other cumulative advantage processes*, Journal of the American Society for Information Science 27 (5) (1976) 292–306. doi:10.1002/asi.4630270505. URL <http://dx.doi.org/10.1002/asi.4630270505>
- [12] R. K. Merton, *The Matthew effect in Science: The reward and communication systems of science are considered.*, Science 159 (3810) (1968) 56–63. doi:10.1126/science.159.3810.56. URL <http://dx.doi.org/10.1126/science.159.3810.56>
- [13] B. T. Hayes, *Follow the Money*, American Scientist (2002). URL <https://api.semanticscholar.org/CorpusID:123614498>
- [14] B. M. Boghosian, M. Johnson, J. Marq, *An H theorem for Boltzmann’s equation for the Yard-Sale Model of asset exchange*, Journal of Statistical Physics 161 (2015) 1339 – 1350. URL <https://api.semanticscholar.org/CorpusID:254697740>
- [15] S. Plaszczynski, G. Nakamura, C. Deroulers, B. Grammaticos, M. Badoual, *Levy geometric graphs*, Phys. Rev. E 105 (2022) 054151. doi:10.1103/PhysRevE.105.054151. URL <https://link.aps.org/doi/10.1103/PhysRevE.105.054151>
- [16] P. L. Krapivsky, S. Redner, *Organization of Growing Random Networks*, Physical Review E 63 (6) (2001) 066123. doi:10.1103/PhysRevE.63.066123.
- [17] B. Mandelbrot, *”sur un modèle décomposable d’univers hiérarchisé: déduction des corrélations galactiques sur la sphère céleste.”*, Comptes Rendus (Paris) 280A (1975) 1551–1554. URL [https://users.math.yale.edu/mandelbrot/web\\_pdfs/comptes\\_rendus\\_79.pdf](https://users.math.yale.edu/mandelbrot/web_pdfs/comptes_rendus_79.pdf)
- [18] B. Mandelbrot, *The Fractal Geometry of Nature*, Freeman, San Francisco, 1983.
- [19] B. Mandelbrot, *The Pareto-Levy Law and the Distribution of Income*, International Economic Review 1 (2) (1960) 79. arXiv:2525289, doi:10.2307/2525289.
- [20] P. Lévy, *Calcul des probabilités*, Gauthier-Villars, Paris, 1925.
- [21] P. Lévy, *Théorie de l’addition des variables aléatoires*, Gauthier-Villars, Paris, 1954.
- [22] W. Paul, J. Baschnagel, *Stochastic Processes*, Springer International Publishing, Heidelberg, 2013. doi:10.1007/978-3-319-00327-6.
- [23] A. Y. Khintchine, *Limit Distributions for the Sum of Independent Random Variables*, O.N.T.I, Moscow (in russian), 1938.
- [24] B. V. Gnedenko, A. N. Kolmogorov, *Limit Distributions for Sums of Independent Random Variables*, Addison-Wesley, Reading, Mass., 1954.
- [25] V. Seshadri, B. J. West, *Fractal Dimensionality of Lévy processes*, Proceedings of the National Academy of Sciences 79 (14) (1982) 4501–4505. doi:10.1073/pnas.79.14.4501.
- [26] A. V. Chechkin, R. Metzler, J. Klafter, V. Y. Gonchar, *Introduction to the Theory of Lévy Flights*, in: R. Klages, G. Radons, I. M. Sokolov (Eds.), *Anomalous Transport*, Wiley-VCH Verlag GmbH & Co. KGaA, Weinheim, Germany, 2008, pp. 129–162. doi:10.1002/9783527622979.ch5.
- [27] B. D. Hughes, M. F. Shlesinger, E. W. Montroll, *Random walks with self-similar clusters*, Proceedings of the National Academy of Sciences 78 (6) (1981) 3287–3291. doi:10.1073/pnas.78.6.3287.
- [28] L. Ozella, D. Paolotti, G. Lichand, J. P. Rodríguez, S. Haenni, J. Phuka, O. B. Leal-Neto, C. Cattuto, *Using wearable proximity sensors to characterize social contact patterns in a village of rural Malawi*, EPJ Data Science 10 (1) (2021) 46. doi:10.1140/epjds/s13688-021-00302-w.
- [29] M. E. J. Newman, *Power laws, Pareto distributions and Zipf’s law*, Contemporary Physics 46 (5) (2005) 323–351. arXiv:cond-mat/0412004, doi:10.1080/00107510500052444.
- [30] E. T. Jaynes, *Information Theory and Statistical Mechanics*, Physical Review 106 (4) (1957) 620–630. doi:10.1103/PhysRev.106.620.
- [31] E. W. Montroll, M. F. Shlesinger, *Maximum entropy formalism, fractals, scaling phenomena, and 1/f noise: A tale of tails*, Journal of Statistical Physics 32 (2) (1983) 209–230. doi:10.1007/BF01012708.
- [32] R. Metzler, J. Klafter, *The random walk’s guide to anomalous diffusion:*

- A fractional dynamics approach, *Physics Reports* 339 (1) (2000) 1–77. doi:[10.1016/S0370-1573\(00\)00070-3](https://doi.org/10.1016/S0370-1573(00)00070-3).
- [33] C. Song, T. Koren, P. Wang, A.-L. Barabási, Modelling the scaling properties of human mobility, *Nature Physics* 6 (10) (2010) 818–823. doi:[10.1038/nphys1760](https://doi.org/10.1038/nphys1760).
  - [34] D. Rybski, S. V. Buldyrev, S. Havlin, F. Liljeros, H. A. Makse, Scaling laws of human interaction activity, *Proceedings of the National Academy of Sciences* 106 (31) (2009) 12640–12645. doi:[10.1073/pnas.0902667106](https://doi.org/10.1073/pnas.0902667106).
  - [35] G. K. Zipf, *Human Behavior and the Principle of Least Effort: An Introduction to Human Ecology*, Addison-Wesley Press, Inc., Cambridge 42. Massachusetts, 1949.
  - [36] A. Delanoë, B. Conein, *Le contrôle de la forme des réseaux par leurs membres : le fil de discussion comme réseau d'interaction*, *SociologieS* (May 2015). doi:[10.4000/sociologies.5046](https://doi.org/10.4000/sociologies.5046). URL <https://doi.org/10.4000/sociologies.5046>
  - [37] R. Heesen, M. Fröhlich, Revisiting the human ‘interaction engine’: Comparative approaches to social action coordination, *Philosophical Transactions of the Royal Society B: Biological Sciences* 377 (1859) (2022) 20210092. doi:[10.1098/rstb.2021.0092](https://doi.org/10.1098/rstb.2021.0092).
  - [38] H.-O. Peitgen, H. Jürgens, D. Saupe, *Chaos and Fractals*, Springer New York, 2004. doi:[10.1007/b97624](https://doi.org/10.1007/b97624). URL <http://dx.doi.org/10.1007/b97624>
  - [39] J.-P. Bouchaud, A. Georges, Anomalous diffusion in disordered media: Statistical mechanisms, models and physical applications, *Physics Reports* 195 (4-5) (1990) 127–293. doi:[10.1016/0370-1573\(90\)90099-N](https://doi.org/10.1016/0370-1573(90)90099-N).
  - [40] S. Jespersen, R. Metzler, H. C. Fogedby, Lévy flights in external force fields: Langevin and fractional Fokker-Planck equations and their solutions, *Physical Review E* 59 (3) (1999) 2736–2745. doi:[10.1103/PhysRevE.59.2736](https://doi.org/10.1103/PhysRevE.59.2736).
  - [41] B. J. West, W. Deering, Fractal physiology for physicists: Lévy statistics, *Physics Reports* 246 (1-2) (1994) 1–100. doi:[10.1016/0370-1573\(94\)00055-7](https://doi.org/10.1016/0370-1573(94)00055-7).
  - [42] T. P. Peixoto, *The graph-tool python library*, figshare (2014). doi:[10.6084/m9.figshare.1164194](https://doi.org/10.6084/m9.figshare.1164194). URL [http://figshare.com/articles/graph\\_tool/1164194](http://figshare.com/articles/graph_tool/1164194)

# A stochastic model of discussion Supplementary Material

S. Plaszczynski, B. Grammaticos, M. Badoual

August 23, 2024

## Contents

<b>S1 The <i>sociopatterns</i> datasets</b>	<b>2</b>
<b>S2 Number of clusters in Levy graphs</b>	<b>2</b>
<b>S3 Amplitude term coefficients</b>	<b>3</b>
<b>S4 Levy clusters distribution in any dimension</b>	<b>3</b>
<b>S5 The Maximum Likelihood Estimator</b>	<b>5</b>
<b>S6 Why dimension 2?</b>	<b>7</b>
<b>S7 Levy flight self-similarity</b>	<b>7</b>

## S1 The *sociopatterns* datasets

As detailed in [1], we focus on 4 datasets from the *sociopatterns* collaboration that we consider as most dissimilar in terms of sociological environment. More complete descriptions are available in the cited references.

The *sociopatterns* collaboration measure interactions between (identified) individuals using RFID proximity sensors [2, 3]. Data is recorded for each pair of participants if they engage in a face-to-face exchange for more than 20 s, which is also the resolution step of the instrument. Data are publicly available from [www.sociopatterns.org](http://www.sociopatterns.org)

1. *hosp*: data collected for 3 days <sup>1</sup> on 75 participants in the geriatric unit of a hospital in Lyon (France) [4]. Most interactions (75%) involve nurses and patients.
2. *conf*: data taken at the ACM Hypertext 2009 ([www.ht2009.org](http://www.ht2009.org)) conference with around a hundred participants (3 days) [5]
3. *malawi*: data were taken in a small village Malawi (Africa) with 86 participants for 13 days. The group consists essentially of farmers [6].
4. *baboons*: data taken at a Primate Center near Marseille (France) with 13 baboons for 26 days [7].

## S2 Number of clusters in Levy graphs

As shown in [1], the mean fraction of clusters follows a power-law function of the scale with a relatively small spread among realizations

$$\frac{N_{clus}}{N} = \frac{A_c}{s^{\alpha_c}} \quad (1)$$

Although we give in the paper the exact formula for the coefficients  $A_c(\alpha)$  and  $\alpha_c(\alpha)$  it still relies on several coefficients (namely  $c(\alpha)$ ,  $\beta(\alpha)$  and  $\gamma(\alpha)$ ) that must be determined from simulations. Instead, we measure here directly their value from the simulations using 1000 realizations of Levy graphs ( $N=100\,000$ ) with fixed  $\alpha$  indices and varying the scale  $s$  between 1 and 10. Figure 1 shows the results and the power-law fits. The resulting parameters are given in Table 1

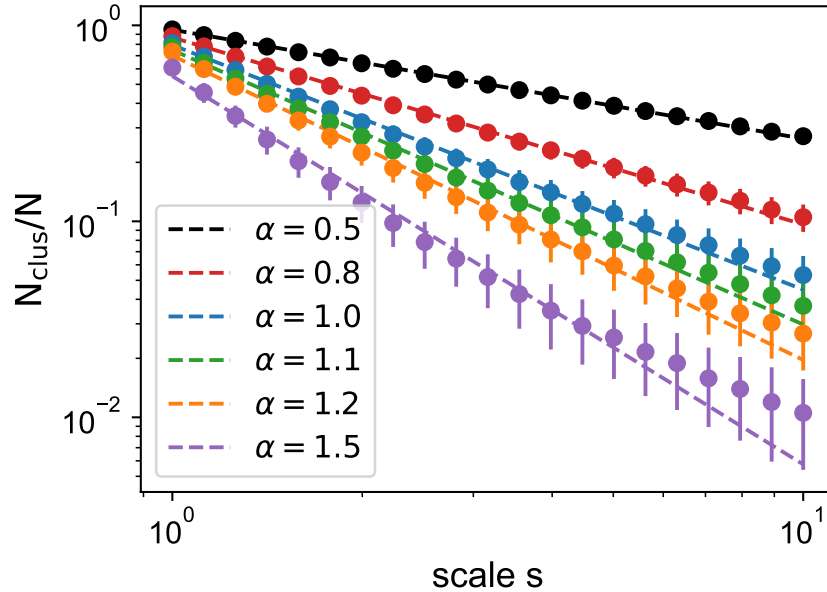


Figure 1: Mean fraction of clusters as a function of the scale as determined from simulations for several  $\alpha$  values. The dashed lines represent the best power-law fits.

<sup>1</sup>we will only consider complete (24 h) day periods.



$\alpha$	$A_c$	$\alpha_c$
0.50	$0.95 \pm 0.01$	$0.56 \pm 0.01$
0.80	$0.87 \pm 0.02$	$0.95 \pm 0.02$
1.00	$0.79 \pm 0.02$	$1.25 \pm 0.04$
1.10	$0.75 \pm 0.02$	$1.40 \pm 0.05$
1.20	$0.70 \pm 0.03$	$1.55 \pm 0.06$
1.50	$0.55 \pm 0.03$	$1.98 \pm 0.09$

Table 1: Coefficients of eq. (1) fitted from the 2D Levy graph simulations (Figure 1) for various  $\alpha$  values.

### S3 Amplitude term coefficients

The amplitude term  $A$  in the distribution of the cluster size is parametrized by

$$A(s) = c/s^\beta. \quad (2)$$

We use simulations to determine  $c$  and  $\beta$  and show the results in dimension 2 on Figure 2.

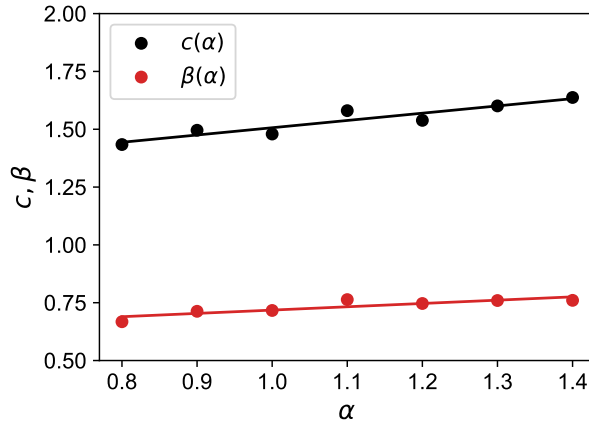


Figure 2: Determination of the values of the  $c$  and  $\beta$  parameters in the  $A(s) = c/s^\beta$  parametrization measured from simulations. The lines show the best linear fits.

### S4 Levy clusters distribution in any dimension

Levy flights may evolve in a space of any dimension  $d$ . One just needs to adapt the angular isotropic part of the jump to the space (a simple algorithm to do it is given in [1]). Although performed in a  $d = 2$  space, most computations in the paper may be adapted to any dimension.

The cluster size distribution is still of the form

$$p(n) \propto \prod_{k=1}^n \left(1 - \frac{A}{k^\gamma}\right) \quad (3)$$

but now, as explained in the paper, we expect

$$\gamma \simeq \alpha/d \quad (4)$$

This is indeed what we observe at large scales in  $d = 5$  simulations as shown in Figure 3.

As in dimension 2, the amplitude term  $A$  is related to the scale through

$$A = c/s^\beta, \quad (5)$$

but this time the  $c$  and  $\beta$  parameters dependency on  $\alpha$  changes with the dimension. For  $d = 5$  we find from simulations (Figure 4) )

$$c = 1.28 - 0.09\alpha \quad (6)$$

$$\beta = 0.40 + 0.45\alpha. \quad (7)$$

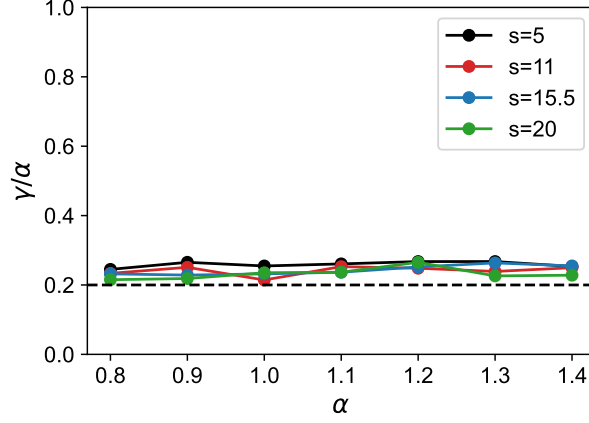


Figure 3: Estimate of the  $\gamma$  parameter from the least square fit of eq. (3) model to Levy graph simulations in a space of dimension  $d = 5$ . The dashed line corresponds to the naive  $1/d$  expectation.

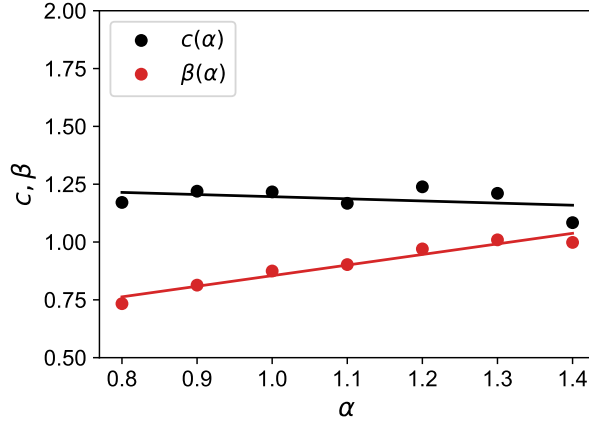


Figure 4: Estimate of the  $c$  and  $\beta$  parameters from the least square fit of eq. (3) model to Levy graph simulations in a space of dimension  $d = 5$ .

If we compare those results to the  $d = 2$  case (Figure 2) we see that the  $c$  dependency on  $\alpha$  has almost vanished while the  $\beta$  one increased. Asymptotically we expect  $\gamma \rightarrow 0$ ,  $A \rightarrow 1$  and  $\beta \rightarrow \alpha$  in order to match the geometric distribution.

The asymptotic approximation for the probability of the cluster size is still valid

$$p(n) \propto \exp\left(-\frac{A}{1-\gamma} n^{1-\gamma}\right), \quad (8)$$

and the CCDF of the cluster size contrast is still

$$p(\delta > x) = \frac{\Gamma[1/\mu, (x\Gamma(2/\mu)/\Gamma(1/\mu))^\mu]}{\Gamma(1/\mu)} \quad (9)$$

but using this time

$$\mu = 1 - \alpha/d. \quad (10)$$

We verify both distributions using simulations on Figure 5.

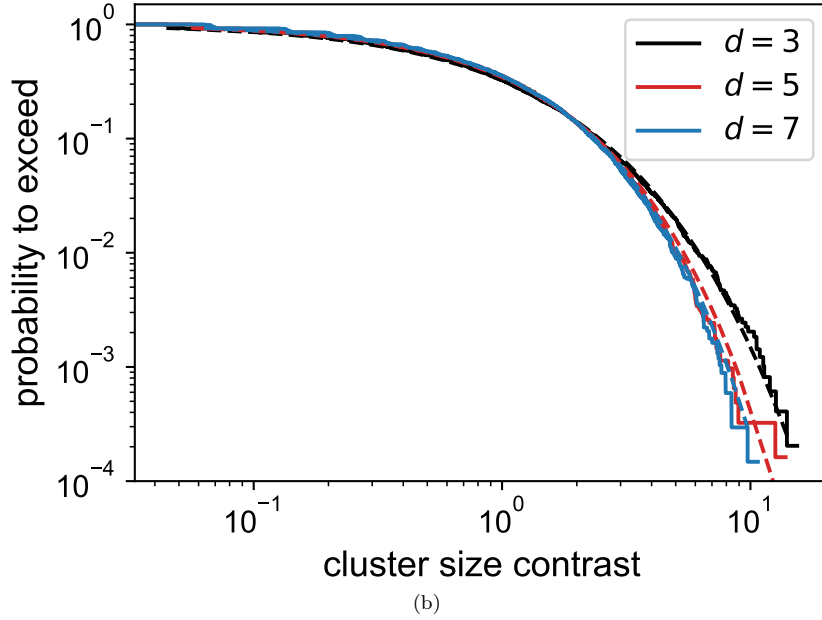
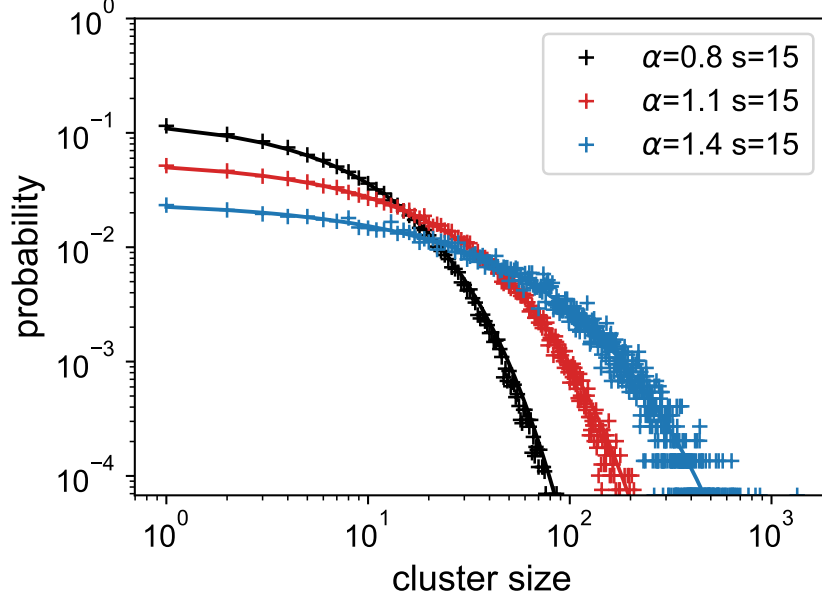


Figure 5: (a) Distribution of the Levy clusters size in a space of dimension  $d = 5$ . Points are obtained from simulations and the line corresponds to the analytical formula eq. (8). CCDF of the Levy cluster size contrast varying the dimension (for  $\alpha = 1.1$ ). The full lines are obtained from simulation while the dashed ones represent the eq. (9) formula.

## S5 The Maximum Likelihood Estimator

The refined distribution of the cluster size contrast of Levy graphs with index  $\alpha$  above some cutoff  $\delta_{min}$  is

$$p(\delta; \alpha) = \frac{g\mu}{\Gamma(1/\mu, (g\delta_{min})^{1/\mu})} e^{(-g\delta)^\mu} \quad (11)$$

$$\text{with } \mu = 1 - \alpha/2, \quad g = f \frac{\Gamma(2/\mu)}{\Gamma(1/\mu)}. \quad (12)$$

The cutoff is important to be sensitive to the tail of the distribution. Indeed the likelihood treats “equally”

all the data points and without it the Levy index is mostly determined by low value samples which are the most numerous in such a distribution.

For a given dataset with samples  $\delta_i > \delta_{min}$ , the likelihood is

$$\mathcal{L}(\alpha) = \prod_i p(\delta_i, \alpha). \quad (13)$$

By maximizing it w.r.t  $\alpha$ , which is traditionally performed by minimizing  $-\log \mathcal{L}$ , one obtains the Maximum Likelihood Estimate (MLE)  $\hat{\alpha}$ .

The factor  $f$  that appears in Eq.(12) is determined from simulations in such a way that the MLE is unbiased. Each dataset defines a set of Levy graphs (of varying size and scale). We fix the index of those graphs to some known value  $\alpha_{true}$  and run 100 realizations per dataset. Each one gives a value of the MLE and we fix  $f$  in order that the mean of the observed values coincide with the input  $\alpha$  value. There is a slight dependency on  $\alpha_{true}$  and by interpolation we obtain a function  $f(\alpha)$  that ensures that the MLE is always unbiased.

We show in Figure 6 an example of the MLE distribution for each dataset with  $\alpha_{true}$  corresponding to the measured data values. The factor  $f$  ensures the mean of those distributions is correct. From the distributions one obtains the standard deviation of the estimator and from the 5 and 95% percentiles a 95% confidence level interval.

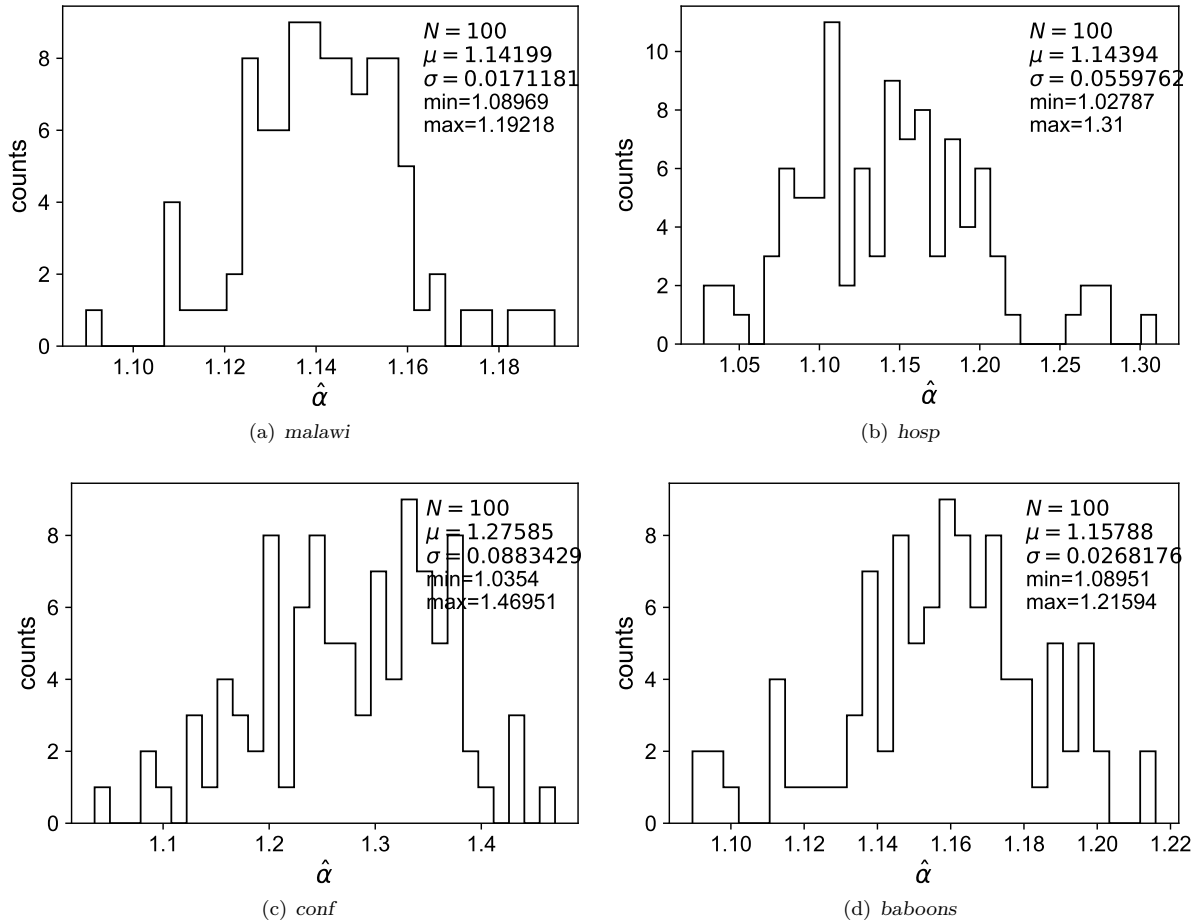


Figure 6: Distributions of the Levy index MLE from simulations. The structure of the graphs is taken from each dataset and the Levy index fixed to  $\alpha_{true} = 1.14(a), 1.14(b), 1.27(c), 1.16(d)$ . The normalization factor  $f$  that appears in eq. (12) ensures that the mean of the distributions coincides with  $\alpha_{true}$ , i.e the MLE is unbiased. Those distributions allow to obtain the precision of the estimator.

## S6 Why dimension 2?

As stated in the paper, the choice of dimension 2 for the Levy walk is only dictated by the data. We have tried other dimensions. Figure 7 shows the result in dimension 3 (using updated  $A_c$  and  $\alpha_c$  coefficients from Sect. S2). Compared to dimension 2 (see paper), the agreement for the *malawi* dataset gets worse in particular at low contrast. Increasing the dimension further degrades the agreement. Indeed the distribution then moves to the geometric one, which has asymptotically a  $\exp(-\delta)$  form (dashed blue line in Figure 7) and is clearly far from the data.

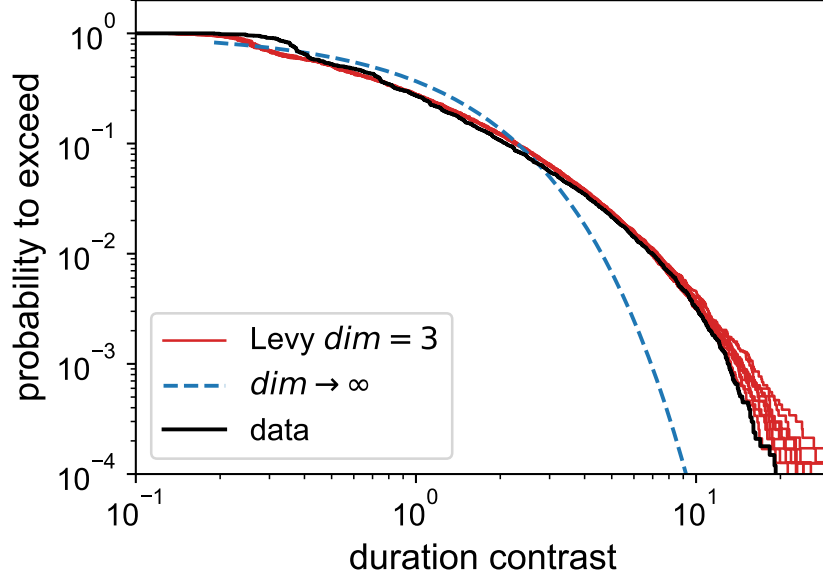


Figure 7: Levy model ( $\alpha = 1.1$ ) in red compared to the *malawi* data (in black) for a Levy walk in a space of dimension 3. Increasing the dimension further, the model converges to the dashed blue line.

## S7 Levy flight self-similarity

To illustrate what the Levy flight self-similarity means, we use simulations. We first generate a 2D Levy flight of index  $\alpha = 1.5$  with  $N = 8192$  points. Then we take only the first half of the points but rescale the coordinates by the factor

$$r = 2^H \quad (14)$$

where the Hurst exponent is given by

$$H = 1/\alpha \quad (15)$$

We repeat the procedure twice and show an example on Figure 8.

The trajectories of this statistical fractal “look the same”. More precisely the  $N$  points are drawn from the very same underlying distribution.

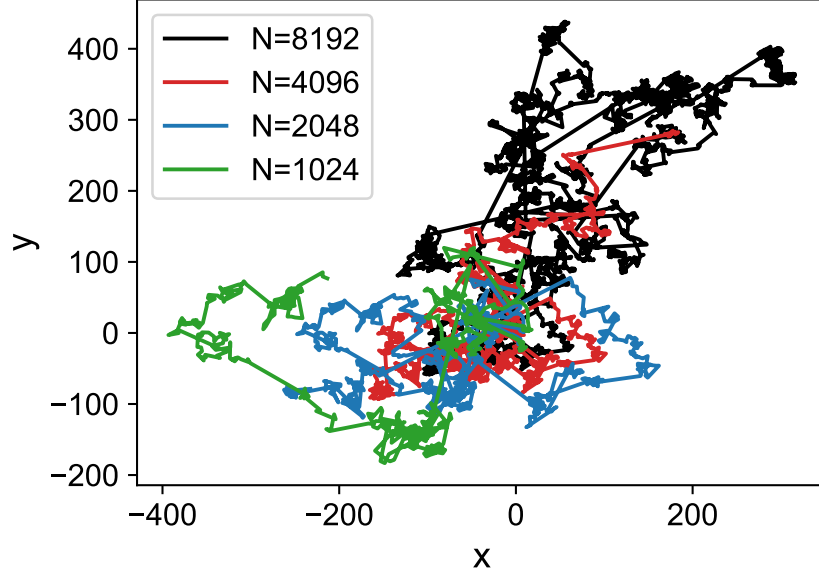


Figure 8: Example of a Levy flight of index  $\alpha = 1.5$  with  $N = 8192$  points (in black). Then one takes the first half of the data ( $N = 4096$  points, in red) and rescale the coordinates by  $2^H$  where  $H = 1/\alpha$ . The procedure is repeated twice.

## References

- [1] S. Plaszczynski, G. Nakamura, C. Deroulers, B. Grammaticos, and M. Badoual. Levy geometric graphs. *Phys. Rev. E*, 105:054151, May 2022.
- [2] Ciro Cattuto, Wouter Van den Broeck, Alain Barrat, Vittoria Colizza, Jean-François Pinton, and Alessandro Vespignani. Dynamics of Person-to-Person Interactions from Distributed RFID Sensor Networks. *PLoS ONE*, 5(7):e11596, July 2010.
- [3] A. Barrat, C. Cattuto, A.E. Tozzi, P. Vanhems, and N. Voirin. Measuring contact patterns with wearable sensors: Methods, data characteristics and applications to data-driven simulations of infectious diseases. *Clinical Microbiology and Infection*, 20(1):10–16, January 2014.
- [4] Philippe Vanhems, Alain Barrat, Ciro Cattuto, Jean-François Pinton, Nagham Khanafer, Corinne Régis, Byeul-a Kim, Brigitte Comte, and Nicolas Voirin. Estimating Potential Infection Transmission Routes in Hospital Wards Using Wearable Proximity Sensors. *PLoS ONE*, 8(9):e73970, September 2013.
- [5] Lorenzo Isella, Juliette Stehlé, Alain Barrat, Ciro Cattuto, Jean-François Pinton, and Wouter Van den Broeck. What’s in a crowd? Analysis of face-to-face behavioral networks. *Journal of Theoretical Biology*, 271(1):166–180, December 2010.
- [6] Laura Ozella, Daniela Paolotti, Guilherme Lichand, Jorge P. Rodríguez, Simon Haenni, John Phuka, Onicio B. Leal-Neto, and Ciro Cattuto. Using wearable proximity sensors to characterize social contact patterns in a village of rural Malawi. *EPJ Data Science*, 10(1):46, December 2021.
- [7] Valeria Gelardi, Jeanne Godard, Dany Paleressompoulle, Nicolas Claidiere, and Alain Barrat. Measuring social networks in primates: wearable sensors versus direct observations. *Proceedings of the Royal Society A: Mathematical, Physical and Engineering Sciences*, 476(2236):20190737, 2020.